DESIGN OF A FORWARD LOOKING SYNTHETIC APERTURE RADAR FOR AN AUTONOMOUS CRYOBOT FOR SUBSURFACE EXPLORATION OF EUROPA

Omkar Pradhan[1], Srikumar Sandeep[1], Albin J. Gasiewski[1],and William Stone[2]
[1]Electrical, Computer and Energy Engineering, University of Colorado, Boulder, CO 80309 USA
[2]Stone Aerospace Inc., Texas, USA

In this paper a forward looking (end fire) synthetic aperture radar (SAR) system is described for the Very deep Autonomous Laser-powered Kilowatt-class Yo-yoing Robotic Ice explorer (VALKYRIE) project. Design and analysis of novel conformal log periodic antennas for the radar and the forward looking SAR ambuguity function is presented. Fabrication and laboratory characterization of the antennas system design and in situ testing of the SAR system are discussed in detail.

I. Introduction

THE VALKYRIE project focuses on the design and development of a field deployable autonomous ice-penetrating cryobot to deploy realistic astrobiology science payloads through substantially thick ice caps. Technology concepts proved in VALKYRIE will lead to surface lander mission concepts to Europa. The need for radar sounding of Europan sub-surface is motivated by the imaging results from the Galileo mission [1]. Radar sounding for Europa in the upcoming Europa fly-by mission has been discussed in [2]. However studying the ocean of liquid water that may lie beneath the icy crust is a signicant engineering challenge and in VALKYRIE these challenges will be met with novel ice-penetrating technology that will allow for carrying science payloads. The SAR system described in this paper will provide critical forward-looking obstacle avoidance capabilities to the VALKYRIE ice-penetrating vehicle. Testing and characterization of the antenna and radar system was carried out at the Stone Aerospace facility in Austin, Texas and on the Matanuska Glacier in Alaska.

II. SAR Antenna and Back end Design

The primary purpose of the VALKYRIE SAR is to provide forward looking obstacle avoidance and ice feature mapping capability for the VALKYRIE cryobot. The development of the SAR system consists of two parts. First is the design of a conformal log-periodic folded slot array (LPFSA) antenna that forms an agile radiating elements for the SAR. The choice of operating frequency and antenna type is influenced by electromagnetic propagation inside ice as well as the mounting space available on the cryobot for the antenna. The antenna is to be flush mounted between the melt head and the sensor suit section (Fig. 1) and must fit on the outer surface of a cylinder with diameter 25.4 cm and within a maximum axial length of 82.5 cm. The maximum radial depth available is 2.035 cm. The active melting of the cryobot creates a thin layer of fresh ice melt water covering the flush mounted antennas. The antenna design must therefore take into account the effects of this dielectric layer. The second part involves the analysis of forward SAR resolution characteristics and design of the radar analog and digital system that includes RF signal generation, transmit-receive isolation and digital SAR data processing using a combination of ARM processor and field programmable gate arrays (FPGA).

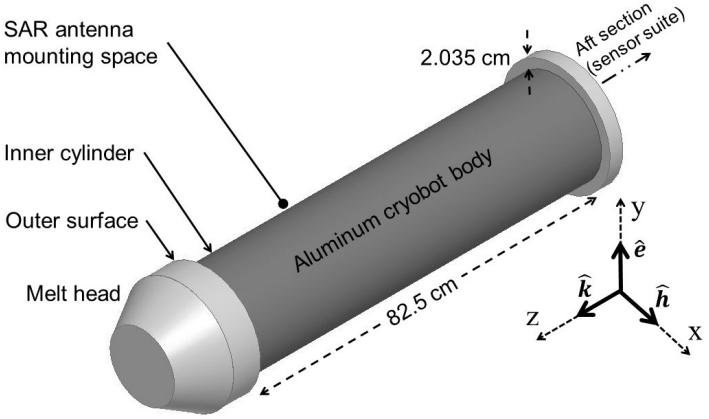

Fig. 1. A scaled model of the section of the cryobot cylinder indicating the volume available for the SAR antenna is shown. The dark grey section has an axial length of 82.5 cm and a radial depth of 2.035. The electric and magnetic field unit vectors ($\hat{e}$) and ($\hat{h}$) and wave propagation unit vector ($\hat{k}$) are shown with bold lines on the cryobot coordinate axis.

A. SAR Antenna Design

The LPFSA [3] is designed by extensive full wave simulations that model the flush mounted antenna and the cryobot along with the melt water layer formed around cylinder. Each conformal folded slot antenna (FSA) element making up the LPFSA is backed by a metallic cavity with small cuts in the corners so as to allow the the surrounding fresh melt water to flood the volume inside. The cavity depth is designed to be equal to a quarter wavelength of the dominant TE_{10} mode inside a fresh water filled waveguide. Two types of feeds are used to interconnect the FSA antennas, a co-planar waveguide (CPW) and a semirigid coaxial cable. The two versions are named CPW-LPFSA and Coax-LPFSA. The dimensions of the CPW and coaxial feeds are chosen so as to have a 50 Ω characteristic impedance. The design constant τ controls the logarithmic periodicity of the resonant antenna elements and is selected to be 0.86 so as to allow a bandwidth of 0.54 to 1 GHz for a five element LPFSA. The spacing constant σ value is selected as 0.75 for the CPW-LPFSA and 0.55 for the Coax-CPW so as to cause constructive

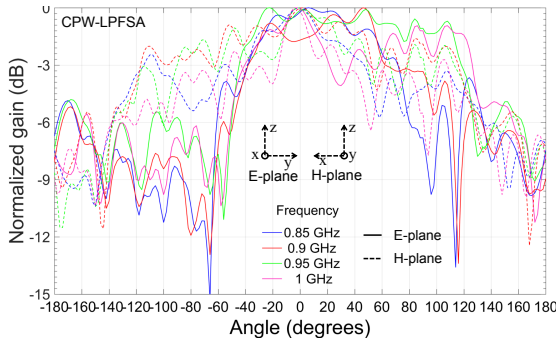

(a)

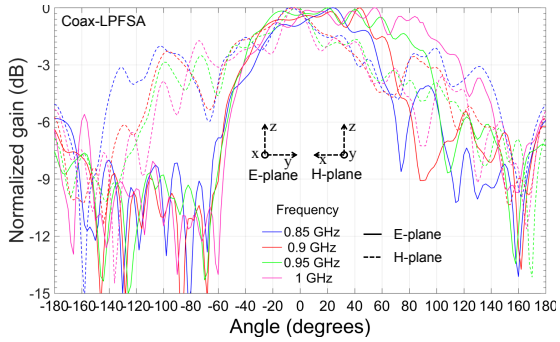

(b)

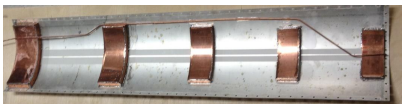

(c)

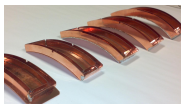

(d)

Fig. 2. In (a) and (b) the E and H plane gain patterns are shown for the chosen design constants τ and σ. A fabricated CPW-LPFSA panel is shown in (c) along with the metallic cavities in (d).

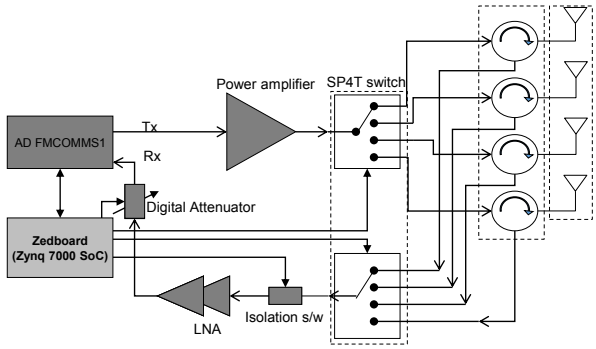

(a)

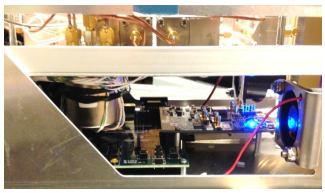

(b)

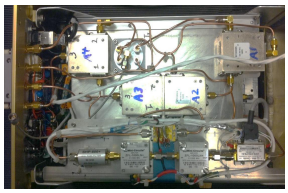

(c)

Fig. 3. Functional block diagram of the SAR transmit/receive system is shown in (a). Images of the (b) Microwave components assembled on the top tray of SAR module and (c) the Zedboard and FMCOMMS1 assembly attached to the bottom tray is shown in.

interference and therefore maximize directivity in the end fire direction. The resulting LPFSA design shows strong main lobes in the endfire direction in both E and H planes as shown in Fig. 2a and 2b. Two LPFSA antennas of each type are fabricated by soldering metallic cavities to the antenna shape printed onto a Rogers RO4003C substrate. The four antennas can be flush mounted onto the cryobot cylinder with each occupying a quarter section of the surface.

B. SAR Back end Design

The SAR back end is designed with commercial off the shelf (COTS) components in a compact assembly to achieve signal generation, transmit/receive and data storage [4]. A functional block diagram of the radar system is shown in Fig. 3a. In the transmit path the power amplifier allows up to 40 dB of gain. The two Single Pole 4 Throw (SP4T) switches enable switching between the antenna elements thus allowing for 16 possible transmit-receive antenna pairs. The digital processing system leverages the sophisticated yet easy to use FPGA development platform called Zedboard which is based on the Xilinx Zynq 7000 all programmable system on chip (SoC) processor. The Zynq SoC uses an ARM+ FPGA architecture core processor. Specifically the Zynq 7000 features a dual-core ARM CortexTM A9 processing system and 28 nm Xilinx programmable logic in a single device. The Zedboard provides a FMC interface to the Analog Devices FMCOMMS1-EBZ radio transceiver card. The FMCOMMS1-EBZ has a 512 MS/s 16 bit digital-analog converter and a 250 MS/s 14 bit analog-digital converter.

C. Forward looking SAR Resolution Analysis

The resolution of a radar can be studied by analyzing its ambiguity function [5]. A radar ambiguity function is a complex valued function, and is a critical component in the systematic search for radar waveforms and processing techniques that can optimize it's resolving capability. The forward SAR geometry shown in Fig (4) can be conveniently represented in the cylindrical i.e. axial (z), radial (ρ) and azimuthal (ϕ) coordinate system. The resolution for the forward SAR system discussed in this paper is analyzed by plotting the normalized magnitude of the ambiguity function for different axial range (z_o) values of a point target as shown in Fig. (4). The ambiguity function analyzed here is a result of aperture synthesis over a 9 m long synthetic aperture. Since in the present analysis a monostatic configuration is considered, the SAR cannot resolve in the azimuthal plane ($x-y$ plane) and therefore the x and y coordinates may be combined into a single radial coordinate ρ which for the point target is fixed at zero. This implies that the target lies directly in front of the radar and therefore is in the so-called end fire direction of the radar antenna. A worsening of the radial resolution is observed from 12 m to 26 m (considering full width of the main lobe) as the axial range of the point target is increased from 50 to 100 m. This effect can be explained by noting that as the axial range increases the phase lag (or lead) of the radar returns from successive radar positions does not change in an appreciable manner therefore reducing the destructive interference required for radial resolution sharpening. However since in the axial direction the target is always visible to the radar antenna an even longer aperture can be synthesized to compensate and thus sharpen radial resolution. The axial resolution remains constant because it only depends upon the width of the transmit pulse for a monotonic transmitter.

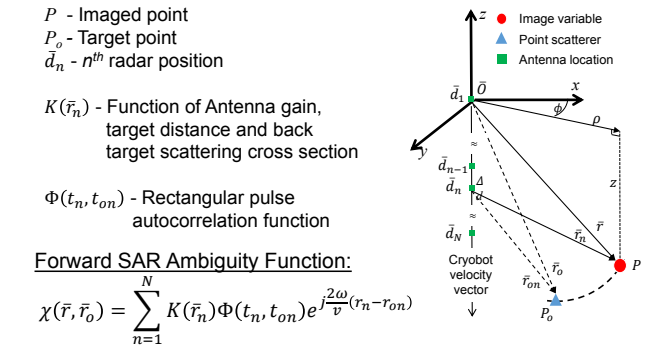

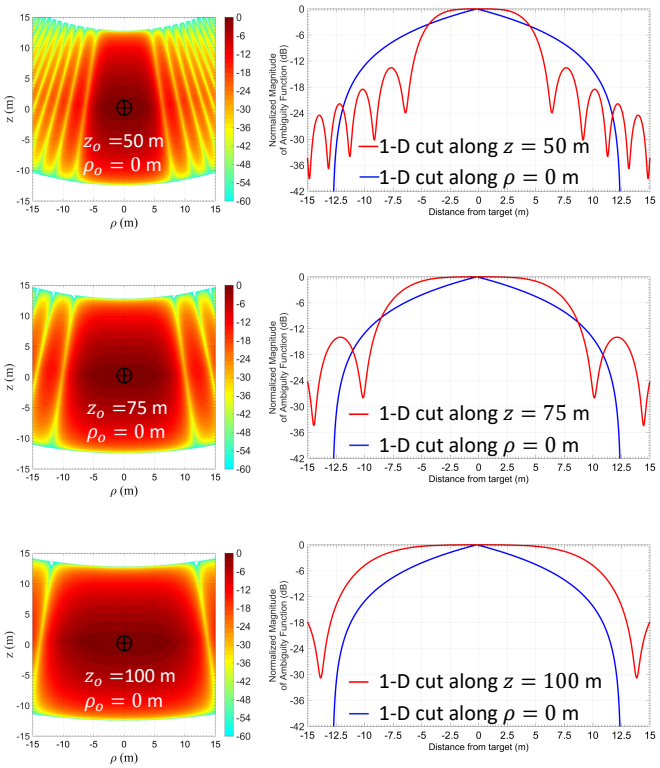

Fig. 4. The forward SAR imaging geometry is shown in (a). The normalized magnitude of the SAR ambiguity function for a point target at an axial range of 50, 75 and 100 m is plotted in the left column. The plots in the right column represent the 1-d cuts of the ambiguity function at the corresponding axial and radial distance.

[]

In this case a pulse width of 1.5 ms is assumed resulting in a axial resolution of 25 m.

III. Antenna Measurements and SAR Image Reconstruction

The atypical environment in which the SAR operates makes it is very difficult if not impossible to emulate an exact representative and at the same time controlled environment for characterizing its antenna and radar performance. Nevertheless outdoor laboratory tests for antenna characterization were carried out at the Stone Aerospace Inc. facility in Austin, Texas. In order to emulate glacial operating conditions a 0.76 m diameter by 1.78 m tall cylinder of ice (weighing ∼1 ton) was prepared and the antenna mounted onto the cryobot was gradually lowered into the ice cylinder along its axis. The test configuration shown in Fig. 5a and 5b facilitated return loss (S_{11}) measurements of

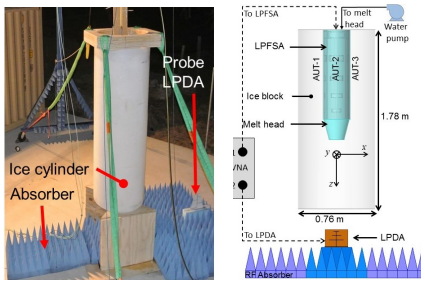

(a) (b)

Fig. 5. (a) Antenna measurement setup at Stone Aerospace Inc. and (b) simulation model of the test setup used in full wave simulations.

the fabricated LPFSA antennas which were then compared with full wave simulations carried out over a variety of melt water thickness values (1,2 and 3 cm) and melt water temperature (0°C, 5°C and 10°C) . The LPDA antenna is translated underneath the cryobot along the x axis in order to measure S_{21} between the LPFSA and the reference probe. The S_{21} is a measure of the E-plane radiation in the end fire direction for the LPFSA under test.

In situ testing of the LPFSA antennas and SAR radar system was carried out on the Matanuska Glacier, Alaska near 61° 42 9.3 N latitude. and 147° 37 23.2 W longitude. Ice boring was achieved using a hot water heater/pump (Hotsy) along with the same melt head attached to the antenna as was used at Stone Aerospace. The antenna structure was suspended from its aft end by a gantry with a pulley arrangement for for deliberate lowering down or raising up of the antenna (Fig. 7a and 7b). A tape measure attached to a fixed point on the gantry was used to accurately measure the depth of the antenna. An older melt hole which was bored in a previous expedition and subsequently filled up with soil is at a distance of 7.5 m from borehole in which the radar was operated. Apart from this other discontinuities in ice also act as scatterers of the transmitted radiation. The measured and simulated antenna S_{11} values are shown in Fig. 7c.

A reconstructed SAR image in terms of the normalized power at the receiver is shown in Fig. 7d. As noted before the cryobot moves downward along the z axis and the x axis is the radial distance from the path of the cryobot. The image is formed by coherent aggregation of the match-filtered received signals over a 5 m long synthetic aperture. The four LPFSA antennas arranged around the cryobot can be used to differentiate between the azimuth coordinates of the radar echos by implementing phase sensitive interferometric processing applied to the received signal at each antenna [6].

IV. Conclusion

In this paper design, analysis and testing of a forward looking synthetic aperture radar for an ice penetrating cryobot vehicle was presented. As part of this work a novel antenna is designed making opportunistic use of the layer of fresh melt water around the vehicle to achieve electrically small resonant cavity. The antenna is characterized and tested in both laboratory and in situ conditions. Resolution of a forward looking SAR system is analyzed using the radar ambiguity function and the the SAR back end hardware is implemented using comercial off-the-shelf components. Finally testing and in situ operation of the radar

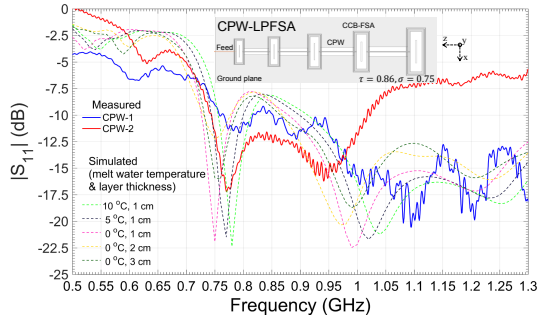

(a)

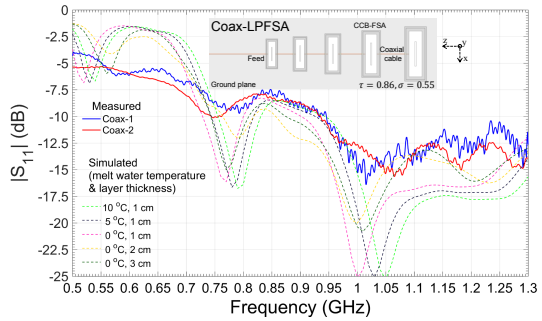

(b)

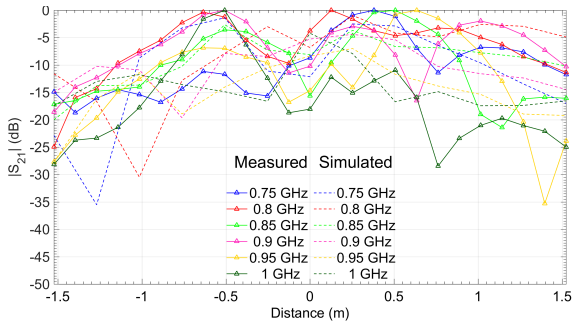

(c)

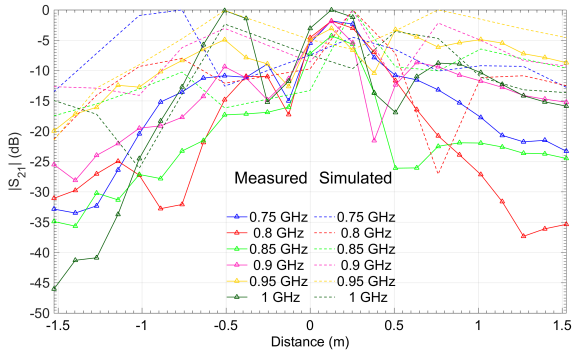

(d)

Fig. 6. Measured S_{11} at Stone Aerospace Inc. are shown for (a) CPW-LPFSA and (b) Coax-LPFSA antennas and are compared with simulated values for various melt water temperatures and layer thickness. The LPDA reference probe is used to measured S_{21} values, plotted along with the simulated values for (c) CPW-LPFSA and (d) Coax-LPFSA antennas.

system including reconstruction of a first light image has also been presented.

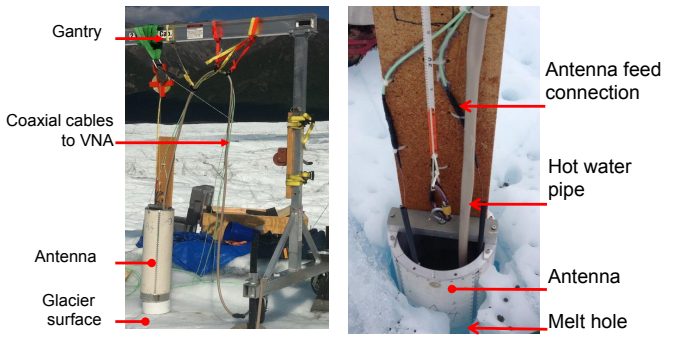

(a) (b)

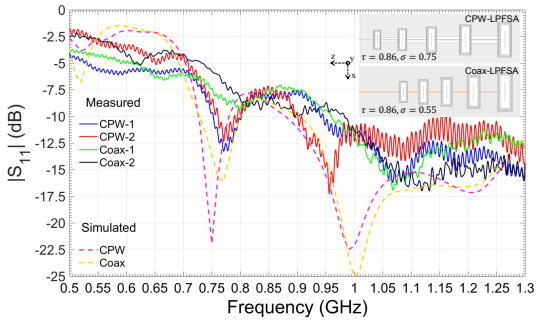

(c)

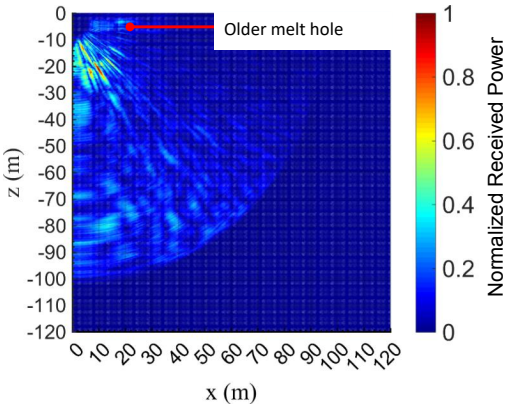

(d)

Fig. 7. (a)Antenna measurement setup on the Matanuska glacier, AK. showing the VALKYRIE cryobot antenna section suspended from the gantry and (b) zommed in photograph of the antenna submerged inside the melt hole. S_{11} measurements are shown in (c) and the reconstructed radar image is plotted in (d)

References

[1] R. Greeley, R. Sullivan, K. C. Bender, M. J. S. Belton, M. Carr, C. Chapman, B. E. Clark, S. A. Fagents, P. E. Geissler, J. W. Head, K. S. Homan, T. Johnson, K. Klaasen, J. Klemaszewski, A. S. Mcewen, J. M. Moore, G. Neukum, and R. T. Pappalardo, "Geology of Europa-Initial Galileo imaging results," *Icarus*, vol. 134, pp. 4–24, 1998.

[2] D. Blankenship, Donald, A. Young, Duncan, B. Moore, William, and C. Moore, John, "Radar sounding of Europa's subsurface properties and processes: The view from Earth." *Univ. Arizona Press*, 2009.

[3] M. Nurnberger, J. Volakis, J. Mosko, and T. Ozdemir, "Analysis of the log-periodic folded slot array," in *Proc. IEEE Antennas Propag. Soc. Int. Symp. URSI Natl. Radio Sci. Meet.*, vol. 2. IEEE, pp. 1282–1285. [Online]. Available: http://ieeexplore.ieee.org/lpdocs/epic03/wrapper.htm?arnumber=407855

[4] E. Zuagg, D. Hudson, and D. Long, "The BYU SAR: A small student-built SAR for UAV operation," in *2006 Int. Geosci. Remote Sens. syposium*, 2006, pp. 411–414.

[5] C. Cook and M. Bernfeld, *Radar Signals An Introduction to Theory and Application*, 2nd ed. Academic Press Inc., 1968.

[6] P. Rosen, S. Hensley, I. Joughin, F. Li, S. Madsen, E. Rodriguez, and R. Goldstein, "Synthetic aperture radar interferometry," *Proc. IEEE*, vol. 88, no. 3, pp. 333–382, mar 2000.